This is the accepted manuscript (postprint) of the following article:
M. Javanbakht, E. Salahinejad, M. Hadianfard, *The effect of sintering temperature on the structure and mechanical properties of medical-grade powder metallurgy stainless steels*, Powder technology, 289 (2016) 37-43.
https://doi.org/10.1016/j.powtec.2015.11.054

The effect of sintering temperature on the structure and mechanical properties of medical-grade powder metallurgy stainless steels

M. Javanbakht [a], E. Salahinejad [b,*], M.J. Hadianfard [a]

[a] Department of Materials Science and Engineering, School of Engineering, Shiraz University, Shiraz, Iran

[b] Faculty of Materials Science and Engineering, K.N. Toosi University of Technology, Tehran, Iran

Abstract

Nanostructured medical-grade stainless steel powders with the chemical composition of ASTM F2581 were liquid-phase sintered with 6 wt.% Mn-Si additive at different temperatures ranging from 1000 °C to 1300 °C. The effect of sintering temperature on the structure and mechanical properties of the samples was investigated. Structural characteristics like porosity, austenite crystallite/grain size, and retained ferrite were analyzed by optical microscopy, Archimedes densitometry, X-ray diffraction, transmission electron microscopy, and ferritometry. The corresponding results showed that residual porosity in the sintered specimens was reduced by increasing the sintering temperature; in contrast, the crystallite/grain sizes were enhanced. The study of the mechanical properties, including hardness, compressive, and abrasive wear behaviors, of the samples indicated that the optimum mechanical properties were obtained for the sintering temperature of 1150 °C, which were superior to those of AISI 316L stainless steel used as a conventional biomaterial.

* **Corresponding author:** *Email addresses*: salahinejad@kntu.ac.ir, erfan.salahinejad@gmail.com

This is the accepted manuscript (postprint) of the following article:
M. Javanbakht, E. Salahinejad, M. Hadianfard, *The effect of sintering temperature on the structure and mechanical properties of medical-grade powder metallurgy stainless steels*, Powder technology, 289 (2016) 37-43.
https://doi.org/10.1016/j.powtec.2015.11.054

Keywords: Nanostructured materials; Sintering; Mechanical Properties

1. Introduction

Austenitic stainless steels, especially type 316L, are widely used as biomaterials, because of low cost compared to other metallic biomaterials, good corrosion resistant and mechanical properties, easy processing, and adequate biocompatibility [1, 2]. Nickel is the main element stabilizing the austenitic phase in this alloy; however, implants made of this alloy sometimes cause allergy, due to nickel ions released in the body [3, 4]. For this reason, nickel-free stainless steels were introduced and are being developed in this critical area [5-7]. Typically, in ASTM standards, two nickel-free medical-grade stainless steels have been recently introduced: ASTM ID: F2229 and ASTM ID: F2581.

One of the processing methods that can be used to fabricate nickel-free stainless steels is powder metallurgy. This route induces porosity in the material, which has been recognized to be desirable for bone implants. Because porosity can improve mechanical interlocking between the host bone and implant, thereby reinforcing the stability of the implant. In addition, porosity reduces the mismatch of the elastic modulus of the implant and surrounding bone and thereby improves its fixation [8, 9]. On the other hand, it is known that by developing nanomaterials, many mechanical properties like strength, fracture and fatigue behaviors are improved. To merge porous biomaterials into nanomaterials, mechanical alloying is widely regarded as a nanostructured powder processing route [10]. The mechanical properties of porous nanostructures are controlled by grain/crystallite size and porosity configuration, suggesting a research area. In this regard, liquid-phase sintering allows a better control of density and porosity for powder metallurgy parts.

This is the accepted manuscript (postprint) of the following article:
M. Javanbakht, E. Salahinejad, M. Hadianfard, *The effect of sintering temperature on the structure and mechanical properties of medical-grade powder metallurgy stainless steels*, Powder technology, 289 (2016) 37-43.
https://doi.org/10.1016/j.powtec.2015.11.054

Concerning powder metallurgy austenitic stainless steels, it has been shown that the decrease of grain size increases yield and tensile strengths and impeded intergranular fracture [11-13]. Regarding liquid-phase sintering, the addition of a Cu-Sn sintering aid to produce high-strength 465 stainless steels has been tested [14]. According to this study, the maximum sintered density was achieved at 1300 °C with 3% of the sintering aid. However, in the nanometric scale, the grain size which is controlled by sintering has a higher effect on the obtained properties, compared to coarse grained materials. The investigation of the effect of sintering time on the mechanical behavior of nanostructured medical-grade nickel-free stainless steels has shown that the role of sintering time in the obtained density at the sintering temperature of 1100 °C is negligible [9]. It has been also shown that by using 6 wt% of a Mn-Si alloy at the sintering temperature of 1050 °C, the maximum density and optimal mechanical properties of nanostructured stainless steels were obtained [15]. However, the effect of sintering temperature was not focused on for nanostructured medical-grade stainless steels. In this study, stainless steels with the composition of ASTM F2581 were synthesized by mechanical alloying, and bulk samples were prepared after adding 6 wt% of the Mn-Si sintering aid. The structure and mechanical properties of the samples were then investigated as a function of sintering temperature.

2. Materials and methods

2.1. Sample preparation

The summary of this research is schematically shown in Fig. 1. Mechanical alloying was used in order to produce stainless steel powders. For this purpose, powders supplied by Merck with the composition of Fe-17Cr-10Mn-3Mo-0.4Si-0.5N-0.2C in wt% (ASTM F2581)

This is the accepted manuscript (postprint) of the following article:
M. Javanbakht, E. Salahinejad, M. Hadianfard, *The effect of sintering temperature on the structure and mechanical properties of medical-grade powder metallurgy stainless steels*, Powder technology, 289 (2016) 37-43.
https://doi.org/10.1016/j.powtec.2015.11.054

were milled in a planetary ball mill with a rate of 500 rpm and a ball-to-powder weight ratio of 20:1 under an argon atmosphere for 48 h in a tempered steel bowl. 4 bearing steel balls of 20-mm and 12 bearing steel balls of 8-mm diameters were used in this work. After alloying, 6 wt.% of Mn-11.5Si pre-alloy powder was added in order to improve the sintering behavior of the stainless steel powders. The pressed samples were then encapsulated in evacuated quartz crystals, then sintered for 60 min at temperatures of 1000 °C to 1300 °C, and immediately cooled in water for keeping the high-temperature austenitic structure at room temperature.

2.2. Structural characterization

Medical-grade stainless steels should have a fully austenitic structure. The existence of magnetic phases (ferrite) in the samples, which is detrimental in medical-grade stainless steels, was checked by ferritometry. To ensure the austenitic formation and to determine its crystallite sizes, X-ray diffraction (XRD, Shimadzu lab X-6000, Cu Kα, step size of 0.02, and step time of 6 seconds) was used, where the results were interpreted by the Rietveld method. A transmission electron microscope (TEM, FEI–Tecnai G2F30) was also used to further analyze the structure of a selective sample. For the TEM sample preparation, a selected sintered specimen was cut into a disc of 3 mm in diameter, ground to approximately 100 μm in thickness, and then electropolished. As the porosity level and density of powder metallurgy samples significantly affect their properties, the size and shape of porosity were also analyzed by optical microscopy. The porosity percentage of the samples was calculated by the Image Analyzer software; also, the density of the samples was measured by the water Archimedes method.

This is the accepted manuscript (postprint) of the following article:
M. Javanbakht, E. Salahinejad, M. Hadianfard, *The effect of sintering temperature on the structure and mechanical properties of medical-grade powder metallurgy stainless steels*, Powder technology, 289 (2016) 37-43.
https://doi.org/10.1016/j.powtec.2015.11.054

2.3. Mechanical characterization

Materials developed for medical applications, especially for orthopedic purposes, should present adequate mechanical properties. In this study, aspects of mechanical properties, including hardness, compressive, and wear behaviors were studied as a function of sintering temperature. Rockwell hardness measurements were conducted on the sintered samples on at least five randomly-located points of the surface, then the average values were reported. For studying the compressive behavior of the samples, compression tests were done at room temperature, based on ASTM-E9. Finally, pin-on-disk wear tests were also performed on the sintered samples at an applied load of 10 N and a velocity of 0.03 m/s to the sliding distance of 400 m. The friction coefficient and wear weight loss were measured and the worn-out surfaces were studied by a scanning electron microscope (SEM, JEOL-JSM 5310). Each sample was tested three times and the average value of wear weight loss was reported.

3. Results and discussion

Based on the ferritometry results (Table 1), which is sensitive to magnetic phases (particularly ferrite in stainless steels), the sintering temperatures of 1050, 1100, 1150, 1200, 1250 °C develop non-magnetic, austenitic stainless steel samples. Lower temperatures produces the α-ferrite phase while higher temperatures develop δ-ferrite, where both are destructive in medical-grade austenitic stainless steel implants [15].

The XRD patterns of the samples sintered at 1000, 1150 and 1300 °C are presented in Fig. 2, showing the typical peaks of the austenitic phase with their miller indices. Indeed, according to the ferritometry results, the amount of ferritic phases in 1000 and 1300 °C is

This is the accepted manuscript (postprint) of the following article:
M. Javanbakht, E. Salahinejad, M. Hadianfard, *The effect of sintering temperature on the structure and mechanical properties of medical-grade powder metallurgy stainless steels*, Powder technology, 289 (2016) 37-43.
https://doi.org/10.1016/j.powtec.2015.11.054

such low that no ferritic phase can be observed in the XRD pattern, while being detectable by the Rietveld analyses. During cooling after sintering, the probability of the eutectoid reaction ($\alpha \rightarrow \gamma + Cr_2N$) essentially exists . However, cooling in water decreases time required for this diffusional transformation and keeps the austenitic phase formed at the high temperature. Also, the M_s temperature of the alloy is lower than room temperature, due to of its high nitrogen percentage; thus, martensitic transformation will not also occur.

Table 1 also lists the austenitic crystallite sizes, measured by XRD, after the sintering process. As can be observed, the crystallites is still in the nanometric scale, although it was expected that during sintering, the nanometric crystals grow because of abundant grain boundary. Grain boundary diffusion is a parameter which controls crystal growth and is a function of grain boundary motion. The parameters affecting the mobility of grain boundary include grain boundary segregation, impurities, porosities, and secondary phase. Reasons for maintaining the nanometric crystals are [16, 17]:

1. Due to the presence of nitrogen and carbon in the alloy accumulated in grain/crystallite boundaries, the grain boundary mobility is significantly retarded.
2. Crystallization of the amorphous phase formed during milling, due to the presence of nitrogen and carbon powders, is slow. Because crystallization requires the rejection of excess nitrogen atoms, which is limited by the small volume of the capsules used for sintering.

The melting point of the additive which is a eutectic alloy with Mn-11.5Si (wt.%) composition, according to the related phase diagram, is 1040 °C [18]. Thus, no liquation occurs at 1000 °C, as the related TEM micrograph (Fig. 3) confirms unmelted zones of the additive, as well some nanometric ferritic regions. Note that previous TEM studies on the samples sintered at the higher temperatures had showed a fully austenitic structure [17, 19].

This is the accepted manuscript (postprint) of the following article:
M. Javanbakht, E. Salahinejad, M. Hadianfard, *The effect of sintering temperature on the structure and mechanical properties of medical-grade powder metallurgy stainless steels*, Powder technology, 289 (2016) 37-43.
https://doi.org/10.1016/j.powtec.2015.11.054

Fig. 4a represents the density of the sintered samples, as measured by the Archimedes method. By increasing the sintering temperature, the higher density was obtained. When the sintering temperature increases from 1000°C to 1050 °C, a sharp increase in density occurs because of the activation of liquid phase sintering and after that by increasing the temperature, the increasing rate of density is lower. Also, Fig. 4b shows that the porosity level decreases with increasing temperature, as calculated by the image analyzer software, which is in good agreement with Fig. 4a, including about the sharp change from 1000 °C to 1050 °C. Indeed, the formation of a liquid phase in the parts, when the additive is melted, makes the major powder wet, penetrates by a capillarity force to pores and develops a region of high diffusivity for sintering densification.

Fig. 5 shows the optical microscopy images of the samples sintered at the different temperatures. By increasing the sintering temperature, porosity contract and their geometry tends to a circular shape. In other word, the porosity becomes smaller, more isolated, and spherical. Another noticeable point is that there are small pores among large pores, except for the samples sintered at 1000 and 1300 °C. According to the ferritometry results (Fig.2), in these two temperatures, some ferrite phase exists in the structure. Ferrite has a BCC structure and the number of atoms in the unit cell of BCC is less than that in FCC. Therefore, the BCC phase scattered in the FCC austenite matrix tends to occupy more volume, inducing compressive stresses to the austenitic crystals and removing the small pores.

Fig. 6 shows the optical image of the sample sintered at 1150 °C, after etching for 60 seconds at the Villela etchant solution (ethanol, hydrochloric acid, and picric acid). This image shows that the Mn-Si rich regions existing among the main particles has been corroded more considerably, compared to the stainless steel particles having a lower tendency to

This is the accepted manuscript (postprint) of the following article:
M. Javanbakht, E. Salahinejad, M. Hadianfard, *The effect of sintering temperature on the structure and mechanical properties of medical-grade powder metallurgy stainless steels*, Powder technology, 289 (2016) 37-43.
https://doi.org/10.1016/j.powtec.2015.11.054

corrosion. Note that the stainless steel alloy is an active-passive alloy due to the presence of chromium, while the Mn-Si additive is a normal alloy without typical passivity. This picture also shows a uniform distribution of the additive among the stainless steel particles, suggesting good wettability and penetration, which is of the main requirements of efficient sintering aids.

Fig. 7 indicates the macrohardness values of the sintered samples, showing an increasing trend from 26 HRC to 36 HRC by increasing the sintering temperature from 1000 °C to 1050 °C. Afterward, the increase in the sintering temperature leads to an increase in the hardness with a lower rate, so that at 1150 °C the maximum hardness (38 HRC) was obtained. From 1150 °C to 1300 °C, the hardness decreases by relatively a low slope and reached 36.7 HRC at 1300 °C. No melting of the additive occurs at the sintering temperature of 1000 °C. By increasing the temperature from 1050 °C to 1150 °C, the additive is melted, its viscosity is reduced; thus, the liquid penetrates to porosity by capillary forces and fills a large portion of them, justifying the increase in hardness (Fig. 7). By further increasing the temperature to 1300 °C, although the previous mechanisms still exist and help to increase the hardness, the increase in the grain/crystallite size is another mechanism occurring and plays a dominant role in the decrease of hardness.

Fig. 8a shows the true stress-strain curves of the samples sintered at the different temperatures. The extracted values of the compressive strength and yield strength of the samples are shown in Figs. 8b and 8c, respectively. The trend observed for both as a function of the sintering temperature is similar to that found for hardness; typically, the most strengths were obtained for the sample sintered at 1150 °C. The strength of porous materials depends on the structure of pores and the yield strength of the matrix determined by the grain size in

This is the accepted manuscript (postprint) of the following article:
M. Javanbakht, E. Salahinejad, M. Hadianfard, *The effect of sintering temperature on the structure and mechanical properties of medical-grade powder metallurgy stainless steels*, Powder technology, 289 (2016) 37-43.
https://doi.org/10.1016/j.powtec.2015.11.054

this study for the different samples. Thus, the maximum strength found for the sample sintered at 1150 °C can be explained by a compromise of porosity and grain size. On the other hand, it has been reported that the yield strength of casting ASTM F2581 and AISI 316L stainless steels is about 482 and 207, respectively [20]. The higher yield strength of the optimum sample prepared in this work can be attributed to its nanometric structure.

Fig. 9a shows the friction coefficient of the sample sintered at 1150 ˚C during the wear test. As can be seen, the friction coefficient is first about 0.15, but after sliding a distance due to wear between the pin tip and sample, the contact surface was rough, the diameter of the pin on the sample was increased, and the friction coefficient increased to 0.4. The other samples showed a similar friction coefficient behavior. The weight loss of the samples due to sliding wear is shown in Fig. 9b. As can be seen, the weight loss for the sample sintered at 1000 °C is more than 1050 °C, due to the absence of liquid-phase sintering below the liquid-phase sintering temperature. Indeed, the reduction in porosity and surface roughness because of the additive liquation is dominant here. Note that the porosity size in the sample sintered at 1000 °C is considerable and some wear debris can penetrate to the porosity, i.e. the real amount of its weight loss should be more than the value reported [21, 22]. By increasing the sintering temperature from 1050 °C to 1250 °C, the weight loss decreases. But the weight loss increases at 1300 °C, due to an increase in the grain size by increasing the temperature and thereby the reduction of hardness. Indeed, the decrease of porosity prevails over the role of the grain size in the wear loss trend in the range of 1050 °C to 1250 °C, in contrast to that of 1250 °C to 1300 °C.

Fig. 10 represents the SEM micrographs of the worn surface of the samples sintered at 1000, 1150 and 1300 °C. Concerning the sample sintered at 1000 °C (Fig. 10a), due to the

This is the accepted manuscript (postprint) of the following article:
M. Javanbakht, E. Salahinejad, M. Hadianfard, *The effect of sintering temperature on the structure and mechanical properties of medical-grade powder metallurgy stainless steels*, Powder technology, 289 (2016) 37-43.
https://doi.org/10.1016/j.powtec.2015.11.054

fact that the pin is harder than the sample, the abrasive wear is dominant, with a small evidence of adhesive wear. However, the dominant mechanism for the samples sintered at 1150 and 1300 °C is the adhesive wear, as can be seen in Fig. 10b. Since the hardness values of the pin and these samples are close, no abrasive wear evidence is seen in these samples.

4. Conclusions

Nanostructured medical-grade stainless steel powder samples were liquid-phase sintered with the addition of 6 wt.% of the Mn-Si sintering aid. Then, their structure and mechanical properties were investigated as a function of sintering temperature. It was found that the mechanical properties, including hardness, yield stress, compressive strength, and wear resistance, were affected by the structural characteristics of porosity and grain size. In this regard, by increasing the sintering temperature from 1000 °C to 1300 °C, the porosity content was reduced, while the grain size was enhanced. By a compromise between the grain size and porosity, the optimum mechanical behavior was found for the sample sintered at 1150 °C for 60 min.

References

[1] J. Disegi, L. Eschbach, Stainless steel in bone surgery, Injury, 31 (2000) D2-D6.
[2] Q. Chen, G.A. Thouas, Metallic implant biomaterials, Materials Science and Engineering: R: Reports, 87 (2015) 1-57.
[3] M. Talha, C. Behera, O. Sinha, A review on nickel-free nitrogen containing austenitic stainless steels for biomedical applications, Materials Science and Engineering: C, 33 (2013) 3563-3575.
[4] M. Li, T. Yin, Y. Wang, F. Du, X. Zou, H. Gregersen, G. Wang, Study of biocompatibility of medical grade high nitrogen nickel-free austenitic stainless steel in vitro, Materials Science and Engineering: C, 43 (2014) 641-648.
[5] K. Yang, Y. Ren, Nickel-free austenitic stainless steels for medical applications, Science and Technology of Advanced Materials, 11 (2010) 014105.

This is the accepted manuscript (postprint) of the following article:
M. Javanbakht, E. Salahinejad, M. Hadianfard, *The effect of sintering temperature on the structure and mechanical properties of medical-grade powder metallurgy stainless steels*, Powder technology, 289 (2016) 37-43.
https://doi.org/10.1016/j.powtec.2015.11.054

[6] M. Sumita, T. Hanawa, S. Teoh, Development of nitrogen-containing nickel-free austenitic stainless steels for metallic biomaterials—review, Materials Science and Engineering: C, 24 (2004) 753-760.
[7] M. Talha, C. Behera, O. Sinha, Effect of nitrogen and cold working on structural and mechanical behavior of Ni-free nitrogen containing austenitic stainless steels for biomedical applications, Materials Science and Engineering: C, 47 (2015) 196-203.
[8] M.M. Dewidar, K.A. Khalil, J. Lim, Processing and mechanical properties of porous 316L stainless steel for biomedical applications, Transactions of Nonferrous Metals Society of China, 17 (2007) 468-473.
[9] E. Salahinejad, R. Amini, M. Marasi, M.J. Hadianfard, The effect of sintering time on the densification and mechanical properties of a mechanically alloyed Cr–Mn–N stainless steel, Materials & Design, 31 (2010) 527-532.
[10] C. Suryanarayana, Mechanical alloying and milling, Progress in materials science, 46 (2001) 1-184.
[11] E. Salahinejad, M.J. Hadianfard, D.D. Macdonald, S. Sharifi-Asl, M. Mozafari, K.J. Walker, A.T. Rad, S.V. Madihally, L. Tayebi, In vitro electrochemical corrosion and cell viability studies on nickel-free stainless steel orthopedic implants, (2013).
[12] T. Onomoto, Y. Terazawa, T. Tsuchiyama, S. Takaki, Effect of Grain Refinement on Tensile Properties in Fe-25Cr-1N Alloy, ISIJ international, 49 (2009) 1246-1252.
[13] H.-b. LI, Z.-h. JIANG, Z.-r. ZHANG, Y. Yan, Effect of grain size on mechanical properties of nickel-free high nitrogen austenitic stainless steel, Journal of iron and steel research, International, 16 (2009) 58-61.
[14] F. Akhtar, Effect of additive Cu-10Sn alloy on sintering Behavior of elemental powders in composition of 465 stainless steel, Journal of Iron and Steel Research, International, 14 (2007) 61-74.
[15] M. Javanbakht, M. Hadianfard, E. Salahinejad, Microstructure and mechanical properties of a new group of nanocrystalline medical-grade stainless steels prepared by powder metallurgy, Journal of Alloys and Compounds, 624 (2015) 17-21.
[16] M. Mendez, H. Mancha, G. Mendoza, J. Escalante, M. Cisneros, H. Lopez, Structure of a Fe-Cr-Mn-Mo-N alloy processed by mechanical alloying, Metallurgical and Materials Transactions A, 33 (2002) 3273-3278.
[17] E. Salahinejad, M.J. Hadianfard, M. Ghaffari, S.B. Mashhadi, A.K. Okyay, Fabrication of nanostructured medical-grade stainless steel by mechanical alloying and subsequent liquid-phase sintering, Metallurgical and Materials Transactions A, 43 (2012) 2994-2998.
[18] A. Handbook, Volume 3: Alloy phase diagrams, ASM international, (1992).
[19] E. Salahinejad, M. Hadianfard, M. Ghaffari, S.B. Mashhadi, A. Okyay, Compositional homogeneity in a medical-grade stainless steel sintered with a Mn–Si additive, Materials Science and Engineering: C, 32 (2012) 2215-2219.
[20] ASTM, Annual Book of ASTM Standards, 13.01: Medical and Surgical Materials and Devices, ASTM International, West Conshohocken, PA, 2001.
[21] H.Ö. Gülsoy, Dry sliding wear in injection molded 17-4 PH stainless steel powder with nickel boride additions, Wear, 262 (2007) 491-497.
[22] K. Kameo, K. Nishiyabu, K. Friedrich, S. Tanaka, T. Tanimoto, Sliding wear behavior of stainless steel parts made by metal injection molding (MIM), Wear, 260 (2006) 674-686.

This is the accepted manuscript (postprint) of the following article:
M. Javanbakht, E. Salahinejad, M. Hadianfard, *The effect of sintering temperature on the structure and mechanical properties of medical-grade powder metallurgy stainless steels*, Powder technology, 289 (2016) 37-43.
https://doi.org/10.1016/j.powtec.2015.11.054

Figures

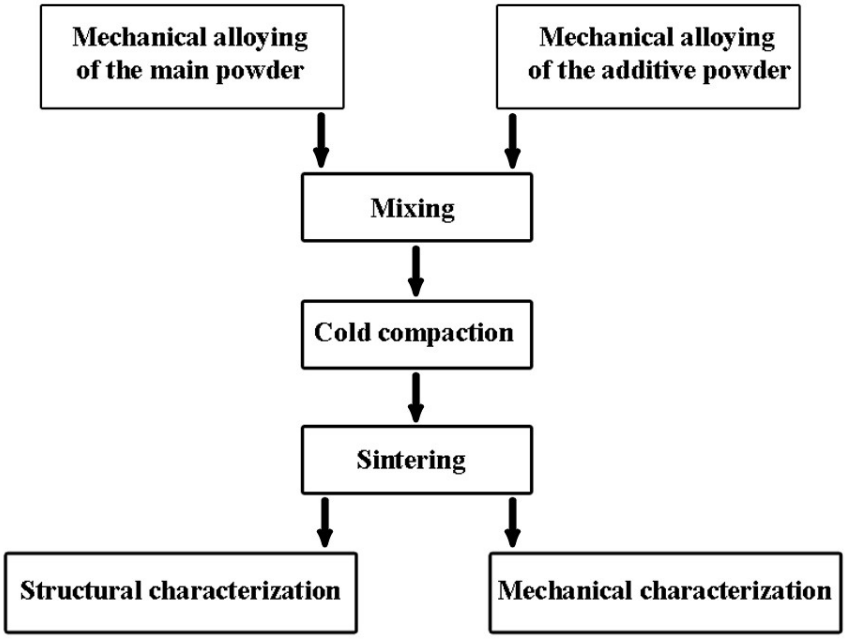

Fig. 1. Schematic representation of this work.

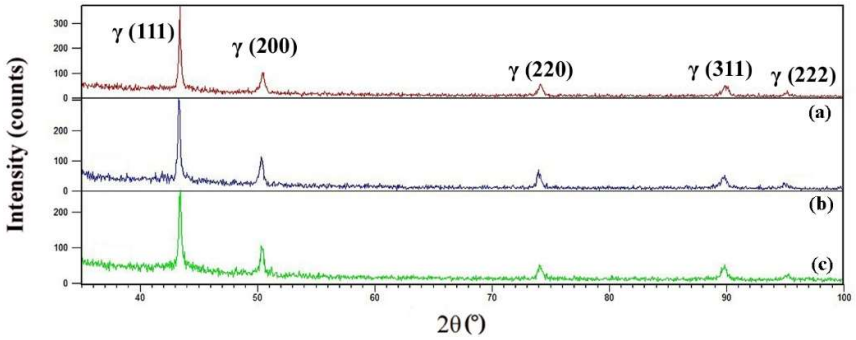

Fig. 2. XRD pattern of the samples sintered at 1000 (a), 1150 (b), and 1300 (c) °C (γ refers to austenite).

This is the accepted manuscript (postprint) of the following article:
M. Javanbakht, E. Salahinejad, M. Hadianfard, *The effect of sintering temperature on the structure and mechanical properties of medical-grade powder metallurgy stainless steels*, Powder technology, 289 (2016) 37-43.
https://doi.org/10.1016/j.powtec.2015.11.054

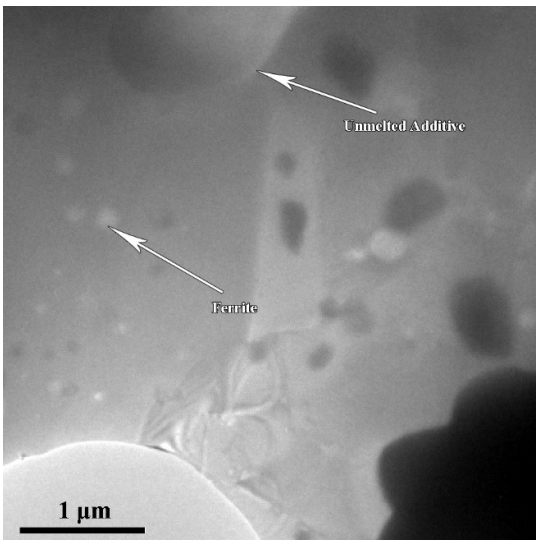

Fig. 3. TEM micrograph of the sample sintered at 1000 °C.

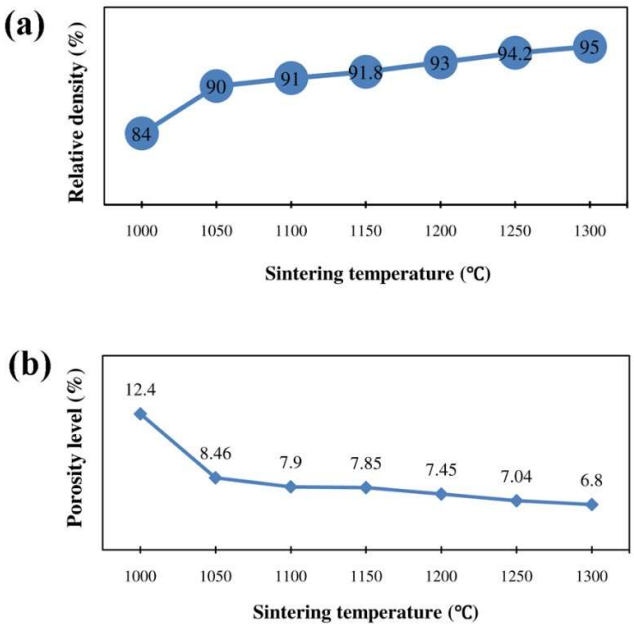

Fig. 4. Relative density (measured by the Archimedes method) and porosity content (calculated by the image analyzer software) of the samples sintered at the different temperatures (experimental error < 1%).

This is the accepted manuscript (postprint) of the following article:
M. Javanbakht, E. Salahinejad, M. Hadianfard, *The effect of sintering temperature on the structure and mechanical properties of medical-grade powder metallurgy stainless steels*, Powder technology, 289 (2016) 37-43.
https://doi.org/10.1016/j.powtec.2015.11.054

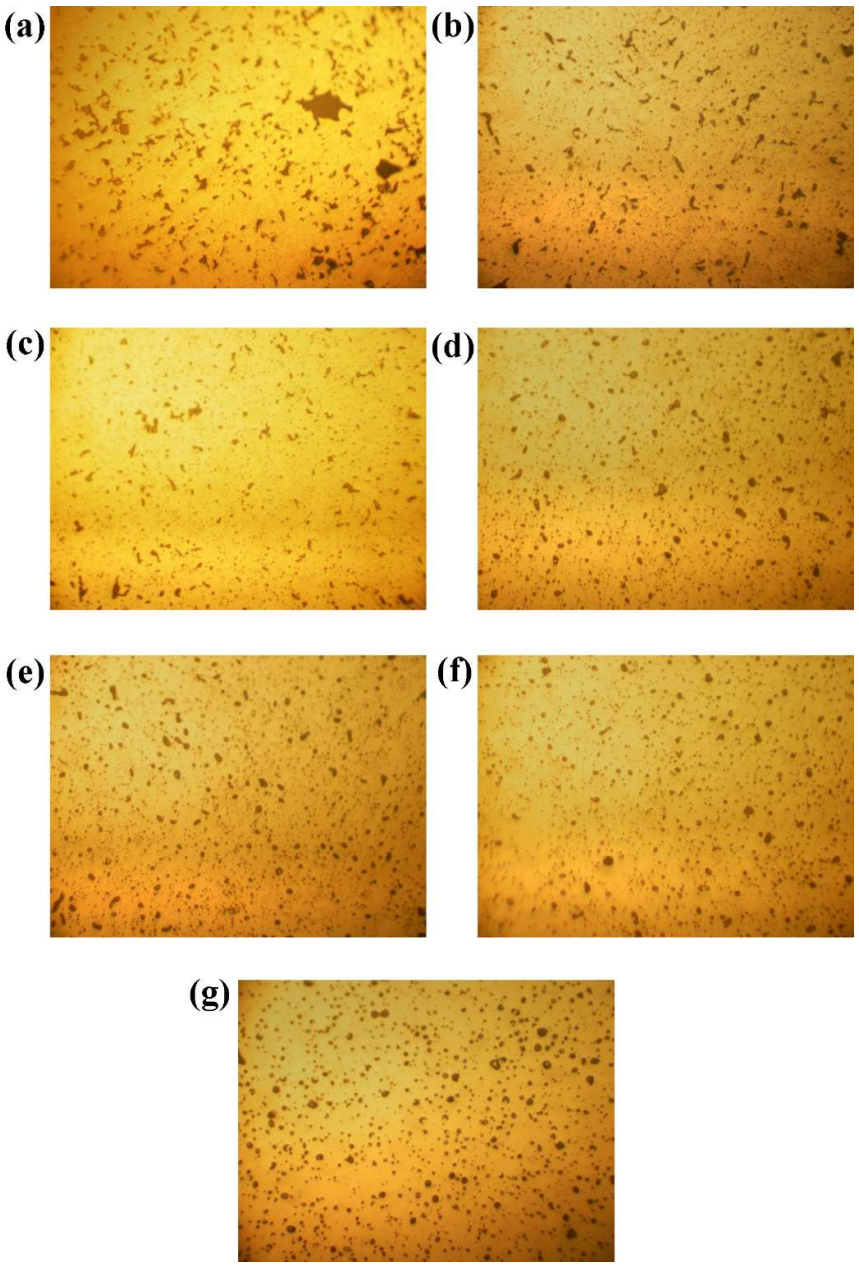

Fig. 5. Optical microscopy images of the samples sintered at 1000 (a), 1050 (b), 1100 (c), 1150 (d), 1200 (e), 1250 (f), and 1300 (g) °C.

This is the accepted manuscript (postprint) of the following article:
M. Javanbakht, E. Salahinejad, M. Hadianfard, *The effect of sintering temperature on the structure and mechanical properties of medical-grade powder metallurgy stainless steels*, Powder technology, 289 (2016) 37-43.
https://doi.org/10.1016/j.powtec.2015.11.054

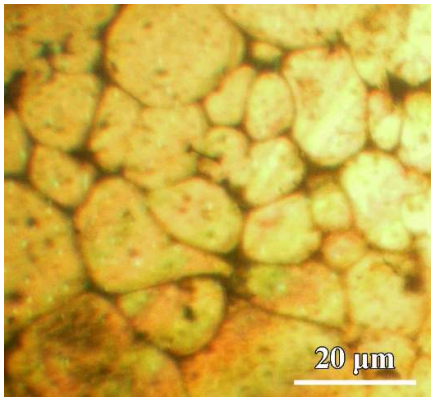

Fig. 6. OM image of the sample sintered at 1150 °C after etching.

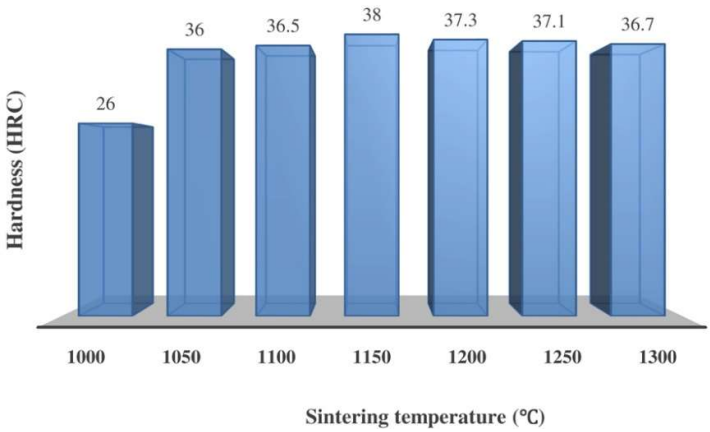

Fig. 7. Macrohardness values of the sintered samples (experimental error < 3%).

This is the accepted manuscript (postprint) of the following article:
M. Javanbakht, E. Salahinejad, M. Hadianfard, *The effect of sintering temperature on the structure and mechanical properties of medical-grade powder metallurgy stainless steels*, Powder technology, 289 (2016) 37-43.
https://doi.org/10.1016/j.powtec.2015.11.054

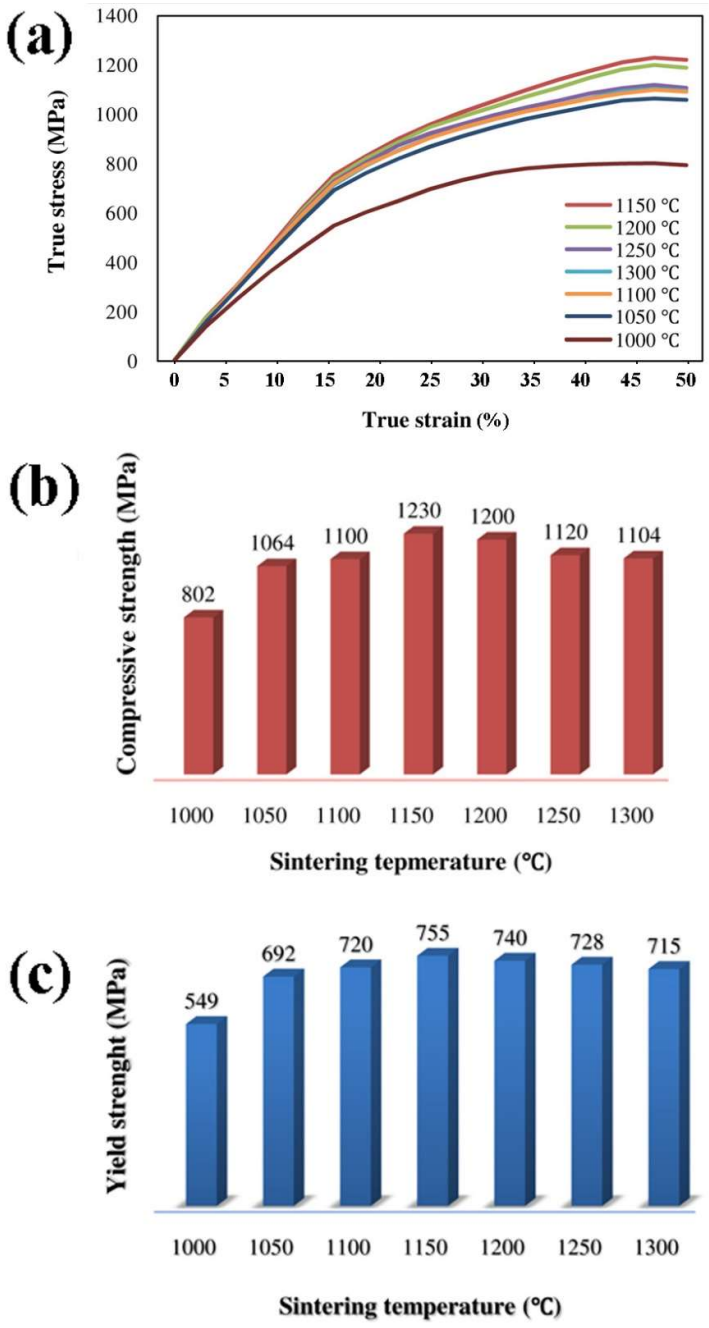

Fig. 8. True stress-strain curve (a), compressive strength (b), and yield stress (c) of the sintered samples (experimental error < 5%).

This is the accepted manuscript (postprint) of the following article:
M. Javanbakht, E. Salahinejad, M. Hadianfard, *The effect of sintering temperature on the structure and mechanical properties of medical-grade powder metallurgy stainless steels*, Powder technology, 289 (2016) 37-43.
https://doi.org/10.1016/j.powtec.2015.11.054

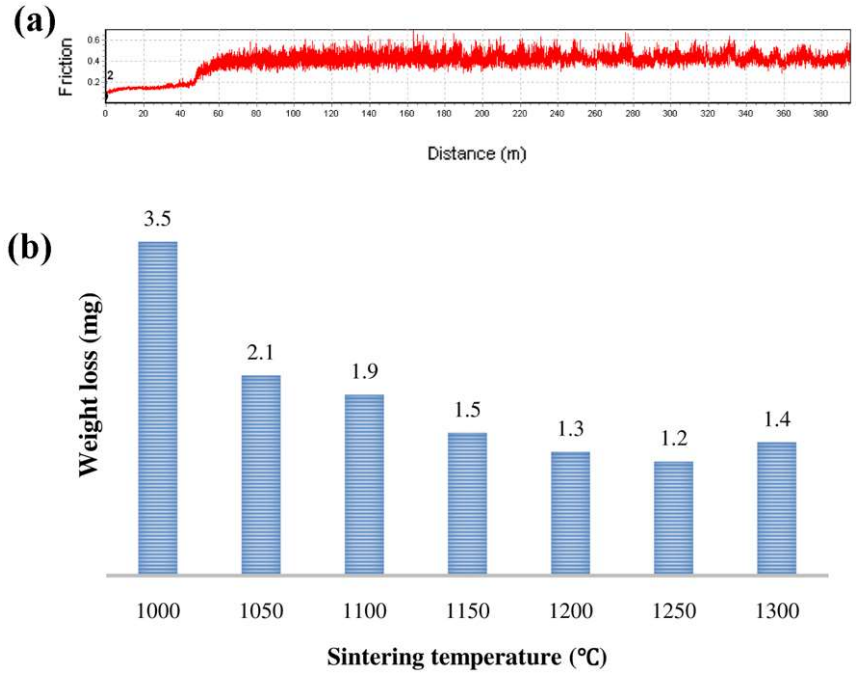

Fig. 9. Friction coefficient diagram of the sample sintered at 1150 °C (a) and wear weight loss values of the samples sintered at the various temperatures (b) (experimental error < 5%).

This is the accepted manuscript (postprint) of the following article:
M. Javanbakht, E. Salahinejad, M. Hadianfard, *The effect of sintering temperature on the structure and mechanical properties of medical-grade powder metallurgy stainless steels*, Powder technology, 289 (2016) 37-43.
https://doi.org/10.1016/j.powtec.2015.11.054

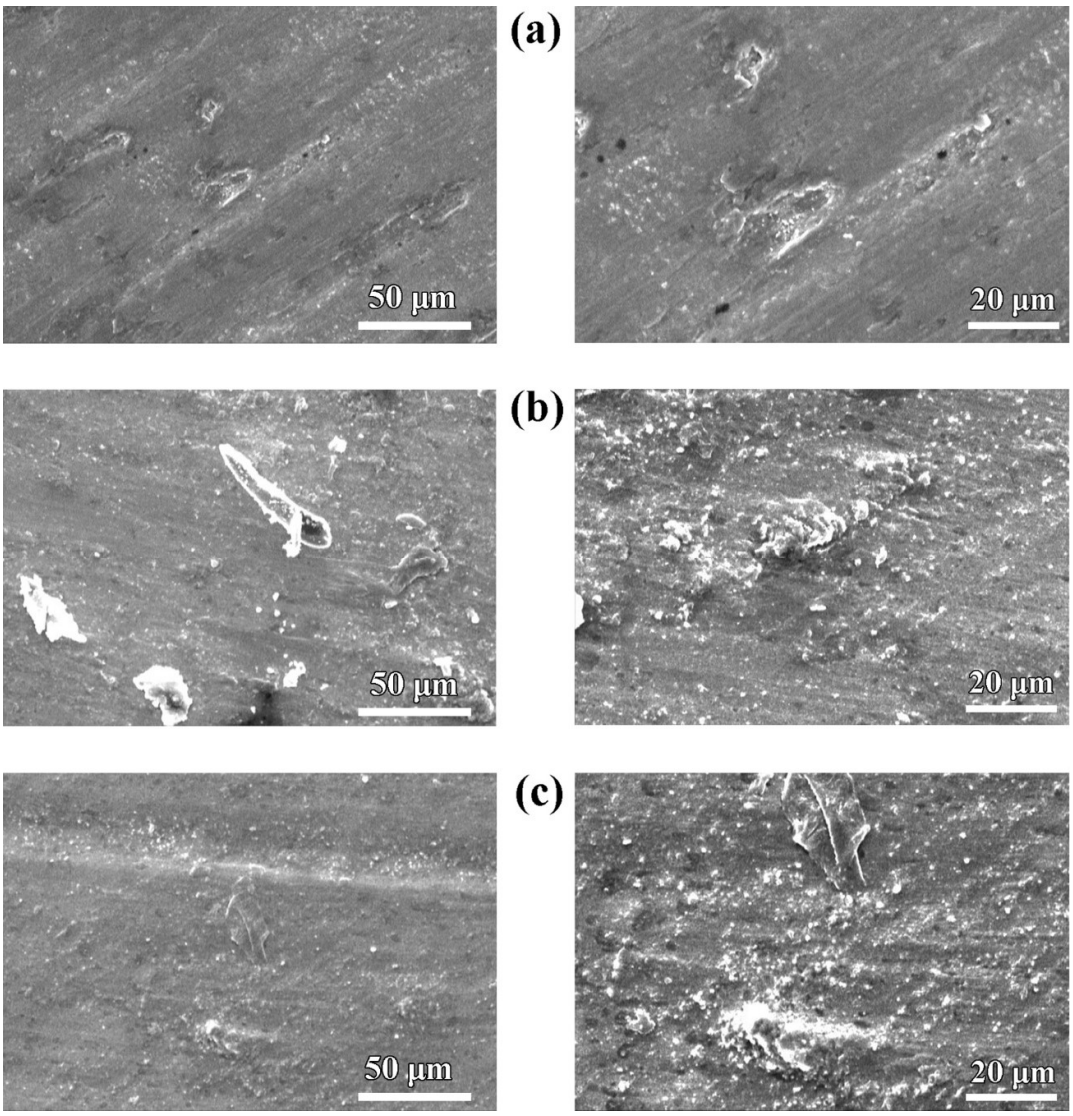

Fig. 10. SEM images of the worn surface of the samples sintered at 1000 (a), 1150 (b), and 1300 (c) °C.

This is the accepted manuscript (postprint) of the following article:
M. Javanbakht, E. Salahinejad, M. Hadianfard, *The effect of sintering temperature on the structure and mechanical properties of medical-grade powder metallurgy stainless steels*, Powder technology, 289 (2016) 37-43.
https://doi.org/10.1016/j.powtec.2015.11.054

Table

Table 1. Some structural parameters of the samples sintered at the different temperatures (experimental error for ferritometry was less than 2%).

Sintering temperature (°C)	Ferrite content (%)	Crystallite size (nm)
1000	3	51
1050	0	*
1100	0	*
1150	0	63
1200	0	*
1250	0	*
1300	6	82

* Not measured.